Oxygen Generating Nanoparticles for Improved Photodynamic Therapy of Hypoxic Tumours.

Yingjie Sheng[1], Heather Nesbitt[1], Bridgeen Callan[1], Mark A Taylor[2], Mark Love[3], Anthony P. McHale[1]* and John F. Callan[1]*.

1.Biomedical Sciences Research Institute, University of Ulster, Coleraine, Northern Ireland, U.K. BT52 1SA. 2. Department of HPB Surgery, Mater Hospital, Belfast, Northern Ireland, U.K. BT14 6AB. 3. Imaging Centre, The Royal Victoria Hospital, Grosvenor Road, Belfast, Northern Ireland, U.K. BT12 6BA

Abstract: Photodynamic therapy (PDT) is a clinically approved anti-cancer treatment that involves the activation of an otherwise inactive sensitisier drug with light, which in the presence of molecular oxygen, generates cytotoxic reactive oxygen species (ROS). As oxygen is a key requirement for the generation of ROS in PDT and given the fact that hypoxia is a characteristic of most solid cancerous tumours, treating hypoxic tumours using PDT can be a challenge. In this manuscript, we have prepared a CaO_2 nanoparticle (NP) formulation coated with a pH-sensitive polymer to enable the controlled generation of molecular oxygen as a function of pH. The polymer coat was designed to protect the particles from decomposition while in circulation but enable their activation at lower pH values in hypoxic regions of solid tumours. The oxygen generating capability of the polymer coated NPs was demonstrated in aqueous solution with minimal oxygen produced at pH 7.4, whereas it increased significantly when the pH was reduced to 6.2. The polymer coated CaO_2 NPs were also observed to significantly increase tumour pO_2 levels ($p<0.05$) in mice bearing ectopic human xenograft MIA PaCa-2 pancreatic tumours with an average increase in tumour pO_2 of 6.5 mmHg in the period 10-30 min following administration. A statistically significant improvement in PDT mediated efficacy ($p<0.001$) was also observed when the particles were administered to mice bearing the same tumours 20 min prior to PDT treatment. These results suggest that the polymer coated CaO_2 NP formulation offers

significant potential as an *in situ* method for oxygen generation to enhance the efficacy of treatments that depend on the presence of oxygen to elicit a cytotoxic effect.

Keywords: Hypoxia, calcium peroxide, Photodynamic Therapy, pancreatic cancer.

1.0 Introduction: Photodynamic therapy (PDT) is a cancer treatment that involves irradiating a photoactive drug with light, in the presence of molecular oxygen, to generate toxic levels of Reactive Oxygen Species (ROS) ultimately resulting in cell death.[1] By carefully controlling light delivery to the target lesion, ROS generation can be localised with high precision in three dimensions sparing healthy surrounding tissue. While the targeted nature of PDT remains its greatest attraction, the technique is significantly limited by the inability of light to penetrate deeply through human tissue.[2] This has restricted PDT to the treatment of superficial lesions and hindered its ability to treat larger solid tumours. The development of near-infrared (NIR) absorbing sensitisers and the emergence of sonodynamic therapy (SDT) promise to overcome this limitation by enabling the activation of sensitisers at greater depths *in vivo*.[3] Combatting hypoxia presents another challenge in the treatment of solid tumours using PDT / SDT as oxygen is a key requirement for the generation of ROS. This is particularly true for tumours of the pancreas[4] and hypoxia is now recognised as an indicator of poor prognosis for many types of cancer.[5,6] Inefficient gas and mass transfer resulting from atypical vascularisation together with elevated oxygen demand by hyper-proliferating tissues results in hypoxia in most solid tumours. Once a hypoxic environment develops in the tumour, cell populations become resistant to many conventional cancer chemotherapeutic agents through a variety of adaptive survival mechanisms. Similarly, for radiotherapy, oxygen has been shown to play a very significant role in enhancing radiation induced damage to nucleic acid in target tissues.[7] One of the major challenges associated with the latter has been to provide oxygen to the target tissues during therapy. A number of approaches have been employed including, hyperbaric oxygen

breathing and breathing pure oxygen or carbogen at atmospheric pressure.[8] Such approaches, however, have delivered limited success and there is still a significant un-met need in this area. We have recently demonstrated that the selective destruction of oxygen loaded microbubbles in the tumour microenvironment using low intensity ultrasound provided a temporary boost in tumour oxygen levels that enhanced the sonodynamic therapy (SDT) treatment of pancreatic tumours.[9] Inspired by these results, we are also focusing on the development of *in situ* oxygen generating nanoparticles as an alternative method to improve tumour oxygenation during PDT.

In this manuscript, we describe the preparation and characterisation of calcium peroxide (CaO_2) nanoparticles that generate molecular oxygen upon decomposition in water. The nanoparticles were coated with a pH-responsive methacrylate based co-polymer containing a tertiary amine residue that protects the nanoparticle core from water at pH values above 7.4. At lower pH values, the tertiary amine unit ionises resulting in dissolution of the polymer coat and exposure of the nanoparticle core to the aqueous environment resulting in oxygen generation (Scheme 1).
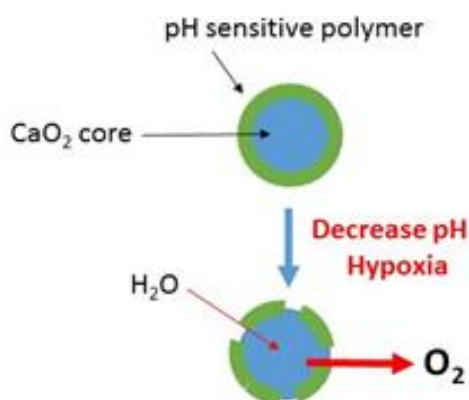
Scheme 1 Schematic illustration of how the polymer coat (green) protects the nanoparticle core (blue) from its aqueous environment at normal pH but at lower pH, the polymer coat dissolves, allowing access to the core by water with the resulting generation of oxygen.

Tumour tissue interstitial fluid is more acidic (pH = ~6.0) than normal tissue, as hypoxia results in the accumulation of acid by inducing the production of energy from glycolysis via the Pasteur effect.[10] This difference in pH has been utilised in numerous pH-responsive cancer therapeutics and diagnostic probes.[11] Here, the pH-responsive polymer coat will limit NP decomposition in the blood and normal tissue while facilitating its decomposition in more acidic cancer tissue. The ability of the resulting oxygen generation to improve oxygenation in hypoxic environments and enhance the PDT-mediated treatment of BxPC-3 pancreatic cancer cells *in vitro* and human xenograft MIA-PaCa-2 pancreatic tumours *in vivo* is demonstrated.

2.0 Materials and Methods

2.1 Reagents and equipment: Calcium chloride, PEG 200, 1M ammonia solution, 35% hydrogen peroxide, sodium hydroxide, phosphate buffered saline (PBS), luminol, methanol, ethanol, hexane, chloroform, Rose Bengal (RB), singlet oxygen sensor green (SOSG), anhydrous tetrahydrofuran (THF), 2-(dimethylamino)ethyl methacrylate, methyl methacrylate, ethyl acrylate and 1,1'-Azobis(cyclohexanecarbonitrile) (ABCN) were purchased from commercial sources at the highest possible grade. BxPC-3 and MIA PaCa cells were obtained from the American Type Culture Collection (ATCC) and matrigel from BD Biosciences,Erembodegem, Belgium. SCID mice (C.B-17/IcrHanHsd-Prkdc^{SCID}) were bred in house. Scanning electron microscopy (SEM) analysis was conducted using an "FEI Quanta" scanning electron microscope while dynamic light scattering (DLS) measurements were performed using a Malvern Zetasizer 3000HSA (Malvern, Worcs., UK). Dissolved oxygen measurements were recorded using a Thermo Scientific™ DO Probe Orion™ 083005MD (Fisher Scientific, Ottawa, ON, Canada) while nanoparticle solutions were mixed using a Silverson homogenizer (Silverson Machines Ltd, Chesham, U.K.). Fluorescence measurements were undertaken using a Cary Eclipse spectrophotometer while 96 well plates were analysed using a Fluostar Omega plate reader. Tumour pO_2 measurements were performed using an Oxylite oxygen electrode sensor (Oxford Optronics, Oxford, UK).

4

NMR spectra were obtained on Varian 500 MHz instrument at 25.0 ± 1 ^{o}C and processed using Bruker software. Mass spectra were obtained using a Finnegan LCQ-MS instrument. Error in measurements was expressed as % standard error of the mean while statistical analysis was undertaken using 2-tailed Students t-test.

2.2 Preparation of uncoated CaO$_2$ NPs: CaO$_2$ nanoparticles were prepared following the method described by Khodaveisi *et al.*[12] Ammonia solution (15.0 mL, 1M) and PEG 200 (120.0 mL, 0.6744 mol) was added to a stirred solution of calcium chloride (3.0 g, 0.027mol) in distilled water (30mL). A solution of 35% H$_2$O$_2$ (15mL, 0.17mol) was then added to the mixture at a rate of 3 drops per minute and the colourless solution stirred for a further 2 h at room temperature. A NaOH solution (0.1 M) was then added until a pH value of 11.5 was achieved when the solution changed to a white coloured suspension. The precipitate was separated by centrifugation (8000g, 5 min) and the resulting pellet washed three times with NaOH (25 mL, 0.1 M). The precipitate was then washed with distilled water until the filtrate pH reached 8.4 and the resulting solid dried *in vacuo* at 80°C for 2 h. The resulting particles were suspended in ethanol and sonicated for 5 minutes. The suspension was passed through a Millex Filter Unit (0.45µm) to isolate larger particles and the filtrate concentrated to dryness providing the uncoated CaO$_2$ nanoparticles as a white powder. The size of the nanoparticles was determined by SEM and DLS.

2.3: Determination of CaO$_2$ content in the uncoated CaO$_2$ NPs: The active CaO$_2$ content of the NPs was determined by reaction with luminol in PBS. A chemiluminescence / concentration calibration curve for the reaction of H$_2$O$_2$ with luminol was performed according to the procedure adopted by Komagoe et al.[13] CaO$_2$ NPs suspended in ethanol (50µL, 35.6µM) were added to a luminol solution (50µL, 10mg/mL in PBS) and the luminescence intensity determined using a plate reader. The CaO$_2$ content was determined by indirectly measuring the number of moles of H$_2$O$_2$ produced (by reference to a calibration graph) from the fixed mass of CaO$_2$ powder and assuming all the available CaO$_2$ was converted to H$_2$O$_2$.

2.4: Determination of singlet oxygen generation: The ability of the CaO_2 NPs to enhance PDT mediated singlet oxygen generation was determined using the singlet oxygen probe SOSG. CaO_2 NPs (2mg) in de-oxygenated ethanol (1 mL) were added to a de-oxygenated PBS solution containing SOSG and RB resulting in final concentrations of 2.5 µM (SOSG), 5.0 µM (RB) and 35.6 µM (CaO_2 NPs). The solutions were then exposed to white light for 5 min (Fenix LD01 LED,50 mW output,113.0 J/cm^2) Control experiments were also undertaken and included (i) CaO_2 NP + light and (ii) RB + light. The intensity of SOSG fluorescence at 525 nm upon excitation at 505 nm was recorded at the beginning and at the end of each experiment.

2.5 In vitro PDT experiments: BxPc3 cells were seeded in a 96 well plate at a density of 5 x 10^4 cells per well and incubated in a hypoxic chamber at 37 °C ($O_2/CO_2/N_2$, 0.1: 5: 94.9, v/v/v) for 3 h. The cells were then treated with either (i) RB or (ii) RB with CaO_2 NPs to reach a final concentration per well of 1µM (RB) and 25µM (CaO_2) respectively. The CaO_2 NPs were initially prepared in EtOH that was diluted 1:1 v/v with PBS (100 µL total volume) immediately before addition to wells containing 100 µL media leading to a total EtOH concentration of 25% v/v .Control wells containing untreated cells or cells treated with vehicle alone (i.e. EtOH / PBS 1:1 v/v 100 µL) were undertaken for comparative purposes. The cells were allowed to incubate with the drug / NPs / vehicle for 5 minutes, the medium was then removed and replaced with fresh media. The cells were then exposed to white light treatment for 30 sec (Fenix LD01 LED,50 mW output,11.3 J/cm^2). Following light treatment cells were incubated for a further 3 h in the hypoxic chamber and then for a further 24 hours under normoxic conditions in a humidified 5% CO_2 atmosphere at 37°C. Cell viability was then determined using a MTT assay.

2.6 Preparation of polymer 1: 2-(dimethylamino)ethyl methacrylate (157.2 mg, 1mmol), methyl methacrylate (100.1mg, 2mmol) and ethyl acrylate (100.1mg, 1mmol) and a catalytic amount of the free radical initiator (ABCN) were dissolved in anhydrous THF (5mL) and placed in a Carious reaction vessel. The contents were then subjected to three freeze-pump-thaw cycles, sealed under vacuum and placed in a Carious oven at 80°C for 72 h. The

contents were removed and hexane (20mL) added to the facilitate precipitation followed by centrifugation for 5 min at 3500g. The supernatant was removed, the pellet containing **1** re-dissolved in anhydrous THF, precipitated again using hexane and centrifuged at 3743 x g. This purification procedure was repeated twice further before the pellet was dried *in vacuo* at 80 ^{o}C and characterised by ^{1}H NMR spectroscopy.

2.7 Coating of CaO$_2$ NPs with polymer 1 to form 1-CaO$_2$ NPs: CaO$_2$ NPs were coated with **1** using a modified single emulsion method.[14] CaO$_2$ NPs (10mg) were dispersed in hexane (10mL) and sonicated for 5 min. The NP suspension was then added dropwise at a rate of 2mL / min to a solution of **1** (100mg, 0.36μmol) in ethanol (40mL) using a Silverson homogeniser at 8000g for 5 min to ensure efficient mixing. After a further mixing period of 6 h, excess solvent was allowed to slowly evaporate and the **1**-CaO$_2$ NPs reconstituted in sterile water. Particle size was then determined using SEM and DLS.

2.8 Dissolved oxygen experiments: For the dissolved oxygen experiments involving the uncoated CaO$_2$ NPs, an ethanol solution containing the NPs (10.0 mg, 24 mmol) was added to 10mL of de-oxygenated PBS solvent. The dissolved oxygen was then measured and recorded every minute using a dissolved oxygen meter. For dissolved oxygen experiments involving the **1**-CaO$_2$ NPs, separate solutions of de-oxygenated water were pH adjusted to pH 7.4 or 6.2. The **1**-CaO$_2$ NPs (2mg) were then added to each solution and the dissolved oxygen measured using a dissolved oxygen meter 3 min following addition. Results were compared against identical solutions in the absence of **1**-CaO$_2$ NPs. Both sets of experiments were repeated in triplicate.

2.9 Solubility of 1-CaO$_2$ NPs with change in pH: The pH of an aqueous suspension containing **1**-CaO$_2$ NPs (2 mg in 10 mL) was lowered from pH 7.4 to pH 6.2 in approximate 0.1 pH increments following the addition of very small aliquots of 0.1 M HCl. Photographs of the resulting suspensions / solutions were taken at pH 7.4, 6.9 and 6.2.

2.9: Determination of tumour pO$_2$: All animals employed in this study were treated humanely and in accordance with licenced procedures under the UK Animals (Scientific

Procedures) Act 1986. The ability of the **1**-CaO_2 NPs to influence tumour hypoxia was examined in a mouse xenograft tumour model of human pancreatic cancer. MIA PaCa-2 cells were maintained in RPMI-1640 medium supplemented with 10% foetal calf serum. Cells were cultured at 37 °C under 5% CO_2 in air. The cells (5×10^6) were re-suspended in 100 µL of Matrigel® (BD Biosciences, Erembodegem, Belgium) and implanted subcutaneously into the rear dorsum of male SCID mice. Tumour formation occurred approximately 5 weeks after implantation and tumour measurements were taken every other day using callipers. Once the tumours had reached an average volume of 254 ± 17 mm^3 calculated from the geometric mean diameter using the equation tumour volume = (W*H*L/2), animals were randomly distributed into two groups (n=3): (i) **1**-CaO_2 NPs and (ii) vehicle only. Following induction of anaesthesia via intraperitoneal injection of Hyponym/Hypnovel (150µl, i.p) of a mixture of 2:1:1; PBS: Hypnorm (0.315 mg/ml fentanyl citrate and fluanisone 10mg/ml, VetaPharma Ltd, U.K.): Hypnovel (10mg/ml midazolom, Roche, UK), the oxygen partial pressure (pO_2) of tumours was recorded using an Oxylite oxygen electrode sensor. A fibre optic probe was inserted into a 21-gauge needle before insertion into the centre of the tumour tissue. The needle was withdrawn and the probe readings allowed to stabilise for 5 minutes. The pO_2 in the tumours was recorded every second for 20 min. 100 µL aliquots of **1**-CaO_2 NPs in a PBS vehicle (2 mg/mL) or PBS alone were administered to the respective groups by tail-vein injection with pO_2 recorded every second for a further 40 minutes. This time period was chosen to avoid the need for re-administering anaesthesia.

2.10 Effect of 1-CaO_2 NPs on PDT efficacy in vivo: Mia-PaCa 2 xenograft tumours were established as described above. Once the tumours had reacted an average volume of 254 ± 17 mm^3 the mice were randomly separated into 4 groups (n=5). Group 1 involved untreated animals, group 2 the PDT only group, Group 3 the **1**-CaO_2 NPs only group and group 4 the PDT + **1**-CaO_2 NPs group. For group 2 mice received an intratumoural injection (100 µL) of Rose Bengal (0.1 mg/mL) in a PBS solvent and the tumour was then exposed to a LED-

8

based white light source for 3 x 3 min treatments (Fenix LD01 LED,50 mW output,205 J/cm^2) with a 1 minute interval between each treatment. Group 3 received a tail vein injection (100 µL) of **1**-CaO_2 NPs in a PBS vehicle (2 mg/mL) while group 4 also received a tail vein injection (100 µL) of **1**-CaO_2 NPs in a PBS vehicle (2 mg/mL) in addition to an intratumoural injection (100 µL) of Rose Bengal (0.1 mg/mL) and light exposure administered 20 min after NP injection using the same conditions as described for group 2. The tumour volume was measured daily over the course of 6 days using callipers.

3.0 Results and Discussion: CaO_2 NPs were prepared following a hydrolysis-precipitation procedure similar to that developed by J. Khodaveiside et al. that utilised $CaCl_2$ as a calcium precursor and polyethylene glycol 200 (PEG200) as a surface modifier. The resulting particles were analysed by SEM and found to be spherical in shape with an average diameter of 116.0 ± 7.6 nm (Figure 1a). However, closer inspection of the particle morphology revealed the appearance of several smaller particles coalesced together to form the larger sized NPs. This was confirmed when an ethanol solution containing the NPs was analysed using DLS where the particle diameter was found to be much smaller at 21.0 nm ± 11 nm. (Figure 1b). The amount of active CaO_2 contained within the NP powder was determined by measuring the luminescence generated when a fixed amount of the NP powder was dissolved in an aqueous luminol solution. The hydrogen peroxide generated from the reaction of CaO_2 with the aqueous medium (Equation 1) subsequently reacts quantitatively with luminol to produce a chemiluminescence signal that is proportional to the amount of hydrogen peroxide present.[15]

$$2CaO_2 + 4H_2O \rightarrow 2Ca(OH)_2 + 2H_2O_2 \rightarrow 2Ca(OH)_2 + 2H_2O + O_2 \qquad \text{Equation 1}$$
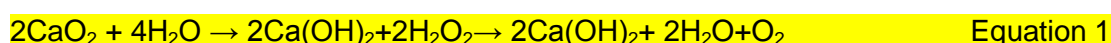
Using this approach, the amount of active CaO_2 present in the NP powder was determined as 44.9 ± 2.3 % with the remaining mass due to excipients such as PEG.
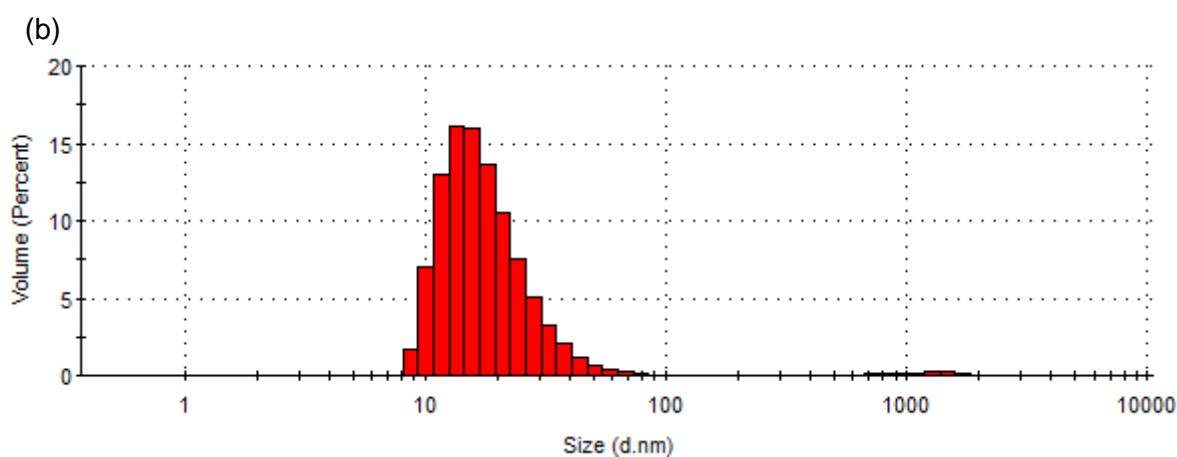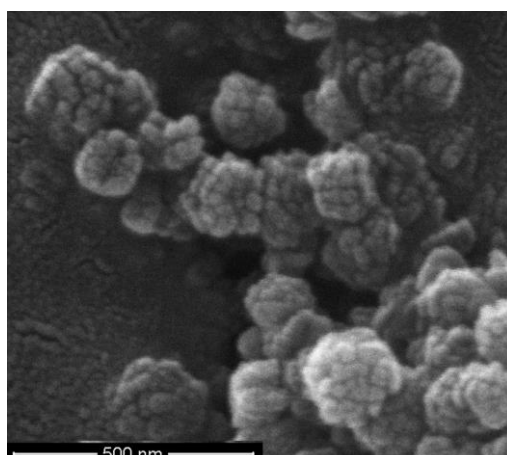
(a)

(b)

Figure 1 (a) Representative SEM image and (b) DLS plot of CaO$_2$ NPs.

To determine the ability of the uncoated CaO$_2$ NPs to generate molecular oxygen upon contact with water and improve oxygen levels in the immediate environment, a simulated hypoxic environment was generated by deoxygenating a solution of PBS (pH = 7.4 ±0.1). A fixed amount of the CaO$_2$ NPs was added to the solution and the amount of dissolved oxygen present in the solution determined as a function of time. The results are shown in Figure 2 and reveal a rapid increase in dissolved oxygen level (37.25%) 10 minutes after NP addition with no further increase observed over the next 10 min suggesting all the CaO$_2$ NPs were used. In contrast, a degassed PBS solution that was exposed to the open atmosphere increased by only 4.10 % over the same time period. These results demonstrate that the CaO$_2$ NPs rapidly decompose when they come into contact with

aqueous medium generating a significant enhancement in the oxygen levels their immediate environment.
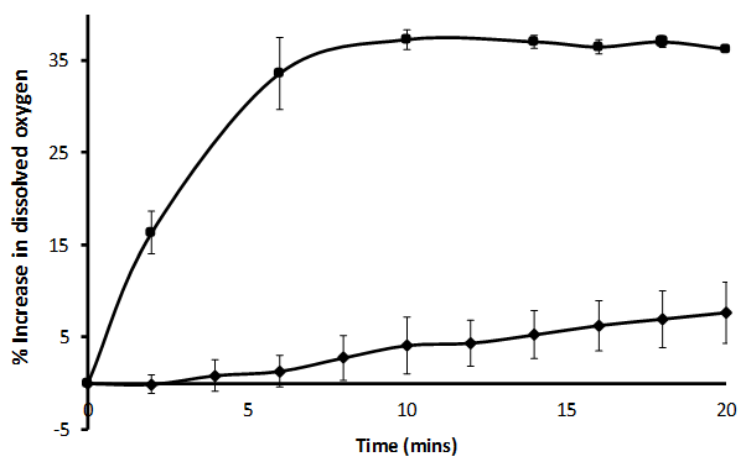
Figure 2 Plot of % increase in dissolved oxygen against time for a solutions of de-oxygenated PBS with (squares) and without (diamonds) addition of CaO_2 NPs.

It is well established that providing oxygen to an excited sensitiser during PDT can enhance the amount of ROS generated, particularly under hypoxic conditions.[16] To identify if the improved dissolved oxygen levels generated by the CaO_2 NPs would also translate to an increase in singlet oxygen quantum yield, the singlet oxygen probe sensor green (SOSG) was utilised. SOSG is inherently non-fluorescent but reacts with singlet oxygen to generate a fluorescent product with the fluorescence intensity being proportional to the amount of singlet oxygen generated. A de-oxygenated PBS solution (2:98; $EtOH:H_2O$) containing SOSG (2.5 µM) and the sensitiser Rose Bengal (5 µM) was prepared and an ethanol solution containing CaO_2 NPs (35.6 µM) added. Immediately, the solution was then irradiated with white light for 5 min at which point the fluorescence intensity at 530 nm was measured. Control experiments in the absence of the CaO_2 NPs (i.e. RB, SOSG and light) and CaO_2 NPs only (i.e. CaO_2 NPs, SOSG, and light) were also conducted for comparative purposes. The results are shown in Figure 3 and reveal a significant increase (324.8%, $p<0.001$) in the amount of SOSG fluorescence observed for the solution containing CaO_2 NPs, RB and treated with light compared to the control experiments, indicating the ability of

11

the NPs to provide oxygen during the photodynamic event and enhance ROS generation in this simulated hypoxic environment.
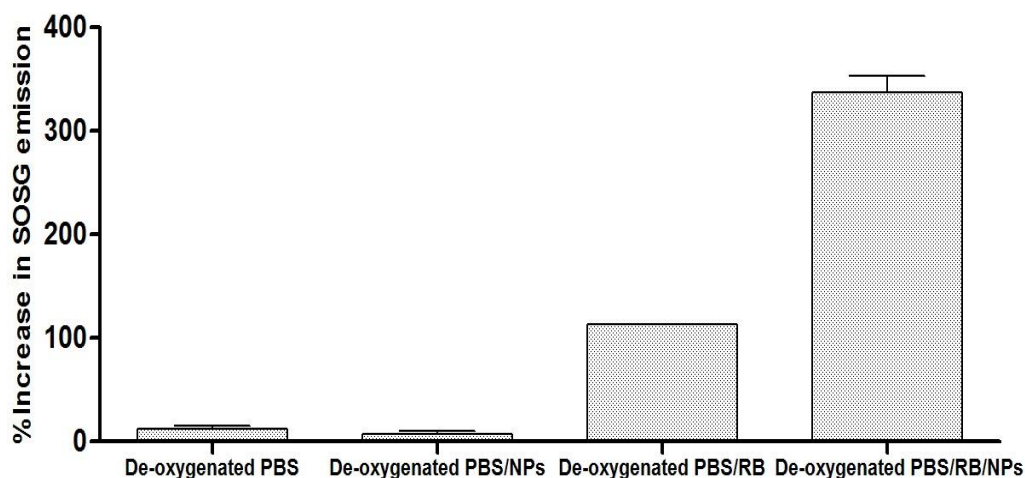

Figure 3 Plot of % increase in SOSG fluorescence at 510 nm for solutions containing (i) degassed PBS (ii) deoxygenated PBS and CaO_2 NPs (iii) deoxygenated PBS and Rose Bengal (RB) and (iv) deoxygenated PBS, Rose Bengal and CaO_2 NPs. Groups (ii)-(iv) also received light treatment.

Having determined the ability of the CaO_2 NPs to improve the light induced ROS generation of Rose Bengal in a simulated hypoxic environment, the next step was to determine if this improved ROS generation would also result in increased Rose Bengal mediated PDT induced toxicity using human BxPC-3 pancreatic cancer cells as a target. The cells were cultured in an anaerobic cabinet ($O_2/CO_2/N_2$, 0.1: 5: 94.9 v/v/v) for 3h to generate a hypoxic environment and then treated with RB (1μM) and incubated for a further 3h under anaerobic conditions. This concentration of RB was identified from previous experiments to have a sub-lethal PDT effect in BxPC-3 cells cultured under hypoxic conditions and would therefore identify any beneficial effect provided by the NPs.[17] The cells were then incubated with an ethanol: PBS (50:50) suspension of the NPs (100 μL, 50 μM) for 5 min before being subjected to light treatment for 30 sec. The NP suspension was then removed, the cells washed with fresh PBS and incubated in fresh medium under normoxic conditions for a further 21 h before cell viability was determined using a MTT assay. The use of a 25%

v/v ethanolic NP suspension in these experiments was not ideal but care was taken to ensure that contact time with the cells was kept to a minimum. We also conducted vehicle only, RB only, light only and NP only controls for comparative purposes. The results are shown in Figure 4 and reveal a significant (p<0.01) reduction in viability for those cells treated with PDT in the presence of CaO_2 NPs (57.9%) compared to PDT treatment alone (25.6%). In addition, there was no observable toxicity exhibited by the nanoparticles themselves at the concentration used in this experiment. These results suggest a synergistic effect between PDT and the CaO_2 NPs in this cell line under these experimental conditions and that treatment of hypoxic BxPC3 with CaO_2 NPs prior to PDT treatment can enhance oxygen levels improving the PDT mediated efficacy.
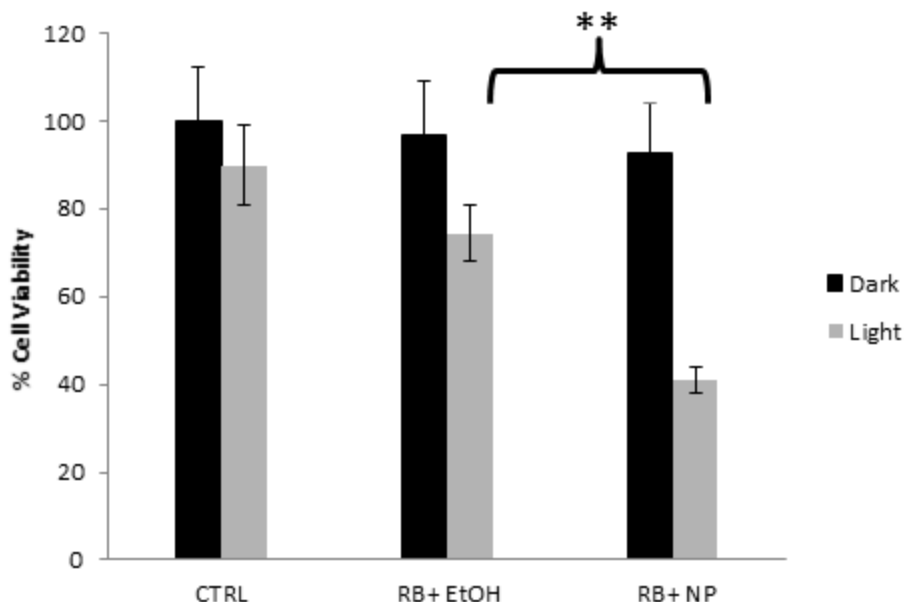
Figure 4   Plot of cell viability for BxPC-3 cells, cultured under hypoxic conditions with (i) no treatment (CTRL dark bar) or after treatment with (ii) light only (CTRL light bar) (iii) RB only in an EtOH vehicle (RB+EtOH black bar) (iv) RB in an EtOH vehicle + light (RB+EtOH light bar) (v) RB + CaO_2 NP in an EtOH vehicle (RB+NP dark bar) (vi) RB + CaO_2 NP+ light in an EtOH vehicle (RB+NP dark bar).

If CaO_2 NPs are to be used *in vivo* it is imperative they remain stable in circulation until taken up by tumour tissue so that inadvertent systemic activation is avoided. In theory, it should be possible to coat the NPs with a polymer that has low aqueous solubility at

physiological pH (i.e. 7.4) but possesses increased solubility in environments where the pH is mildly acidic, as is the case in tumour extracellular fluid (pH = ~ 6.2). We prepared terpolymer **1**, similar in structure to Eudragit E, by the free radical co-polymerisation of 2-(dimethylamino)ethyl methacrylate, methylmethacyrlate and ethylmethacrylate in a 2:1:1 ratio. Eudragit E has been shown to suppress drug release at pH 7.4 when used as a tablet coating but rapidly dissolves in acidic medium to release the active drug.[18] Like Eudragit E, **1** contains a tertiary amine side chain making it possess low aqueous solubility as the free base but become soluble once ionised.[19] The successful preparation of **1** was confirmed by ^{1}H NMR spectroscopy with the stacked spectra of each monomer and **1** shown in Fig 5. The olefinic protons present in the spectra of the monomers between 5.5 and 6.5 ppm were not present in **1** indicating they had been successfully polymerised to form the backbone of **1**. In addition, the peaks were much broader in the spectrum of **1** than in the monomers which is characteristic of protons in or near the backbone of polymers due to an ineffective averaging of their chemical shift anisotropies.[20]
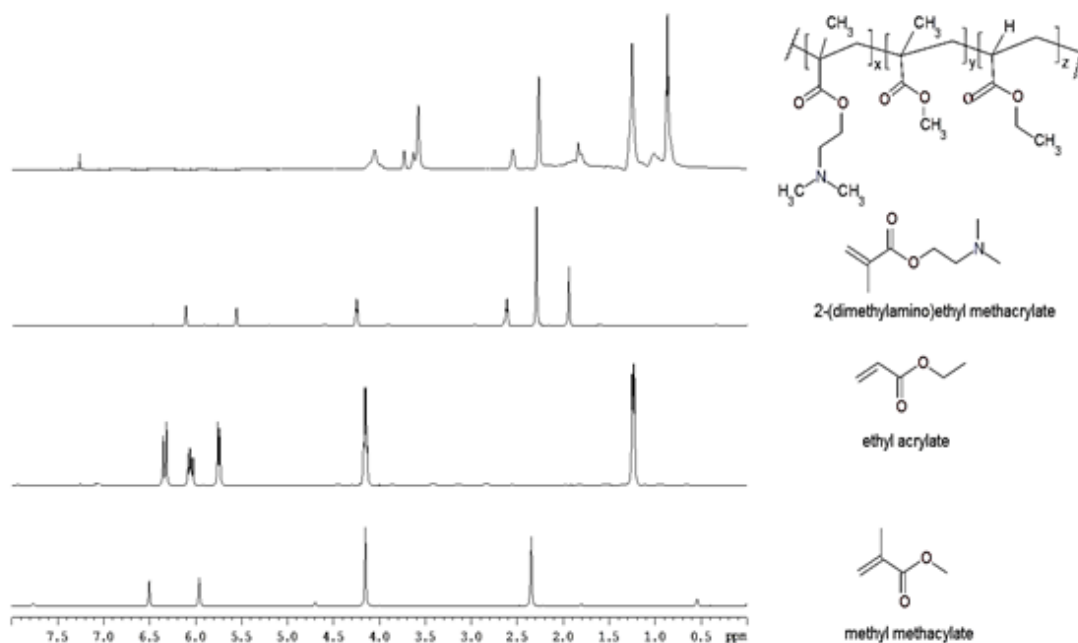
Figure 5 Stacked ^{1}HNMR spectra of (i) methyl methacrylate (ii) ethyl acrylate (iii) 2-(dimethylamino)ethyl methacrylate and (iv) pH responsive polymer **1**.

1 was then used to coat the CaO_2 NPs using a modified oil-in-water emulsion technique. A SEM image of the resulting **1**-CaO_2 NPs is shown in figure 6a and again reveals spherical particles with an average diameter of 248 ± 17 nm which was similar to the hydrodynamic diameter (278 ± 71 nm) determined by DLS.
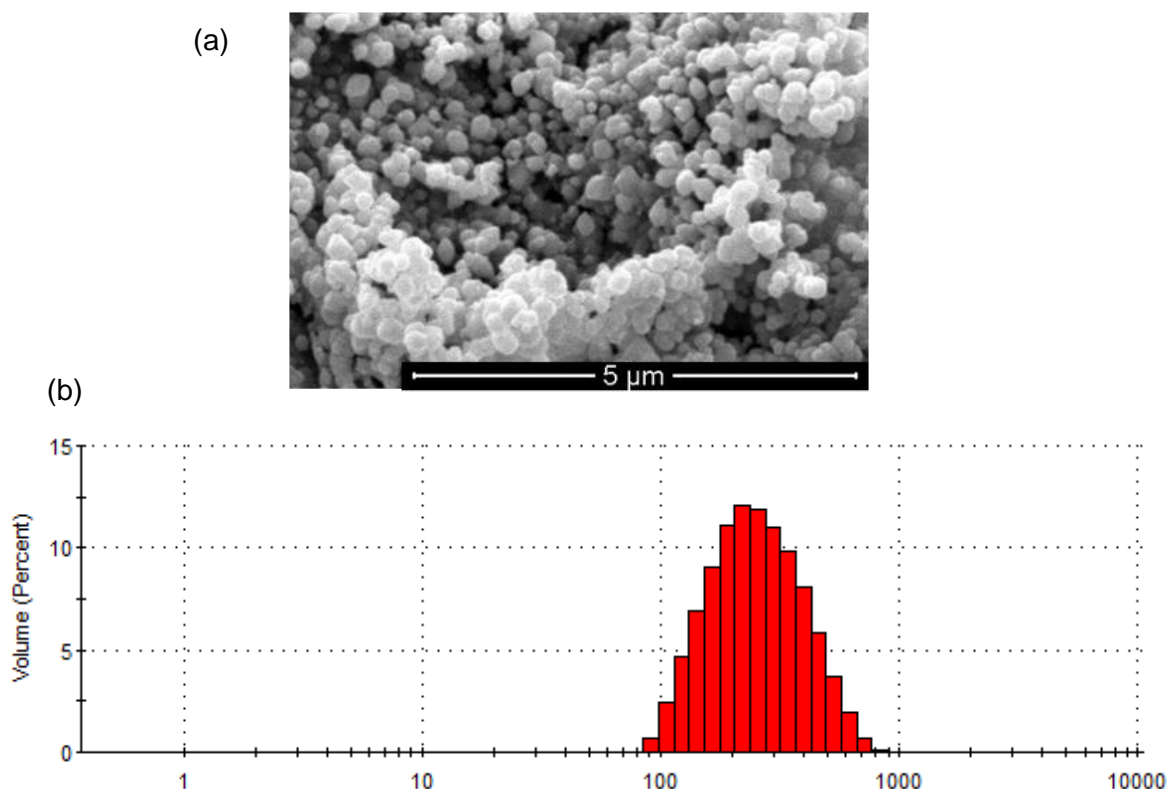
(a)

(b)

Figure 6 (a) SEM image and (ii) DLS plot of **1**- CaO_2 NPs.

The ability of the **1**-CaO_2 NPs to generate oxygen as a function of solution pH was determined by monitoring the increase in dissolved oxygen. Degassed aqueous solutions containing **1**-CaO_2 NPs (1 mg/mL) were pH adjusted to either pH 7.4 or pH 6.2 and the change in dissolved oxygen measured at each pH 5 minutes later. The results are shown in figure 7 and reveal a 45% increase in dissolved oxygen at pH 6.2 compared to only 7% increase at pH 7.4. This increase in dissolved oxygen results from dissolution of the polymer

coat at lower pH that exposes the CaO_2 core to the aqueous environment. Indeed, when an aqueous suspension containing **1**-CaO_2 NPs was pH adjusted from pH 7.4 to pH 6.2, the visual appearance changed from a milky suspension to a more transparent colloidal suspension. These results suggest that the **1**-CaO_2 NPs should remain stable in the systemic circulation at pH = 7.4 but become activated to release O_2 when in the more acidic tumour microenvironment.
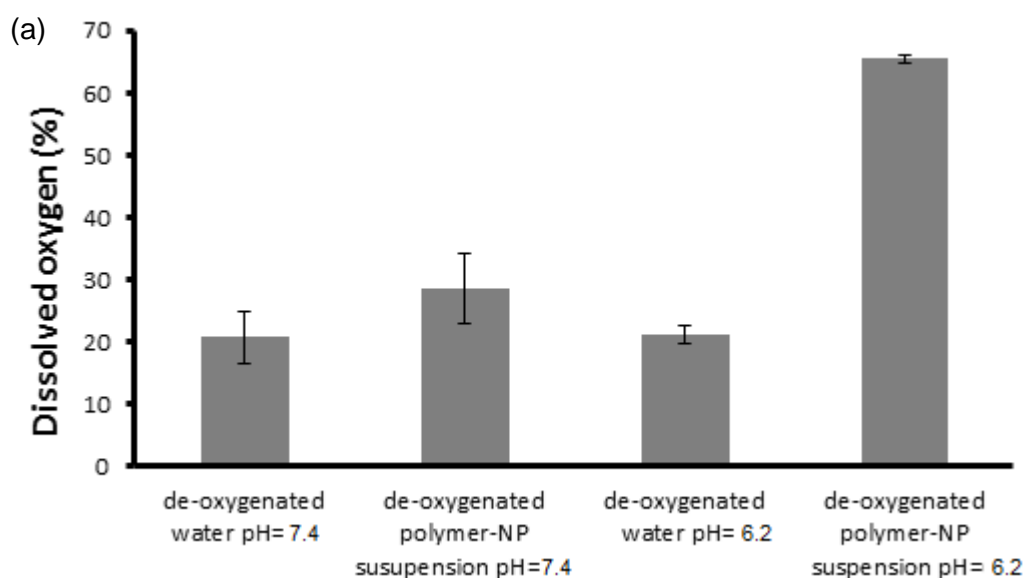
Figure 7 (a) Plot of % dissolved oxygen for solutions of de-oxygenated water at pH 6.2 and pH 7.4 in the absence and presence of **1**-CaO_2 NPs. (b) Photographs showing an aqueous suspension of the polymer coated NPs at pH 7.44, 6.88 and 6.19.

To determine the ability of the **1**-CaO$_2$ NPs to enhance tumour oxygenation in an *in vivo* model, ectopic human xenograft MIA PaCa-2 tumours were established in SCID mice. The MIA-PaCa-2 model is known to form hypoxic tumours and has previously been used in therapeutic efficacy experiments involving hypoxia activated prodrugs.[21] Unlike the BxPC-3 cell line, MIA PaCa-2 cells also express the KRAS mutation making it a more representative model of the disease *in vivo*. Once the tumours reached an average volume of 254 ± 17 mm^3, the mice were separated into two groups (n=3). The treatment group received a tail vein injection of the **1**-CaO$_2$ NP suspension in a PBS buffer vehicle (pH 7.4 ± 0.1), with the control group receiving the same volume of vehicle only. Tumour pO$_2$ readings were recorded using an Oxylite oxygen electrode sensor for 20 min before and 40 min after injection.
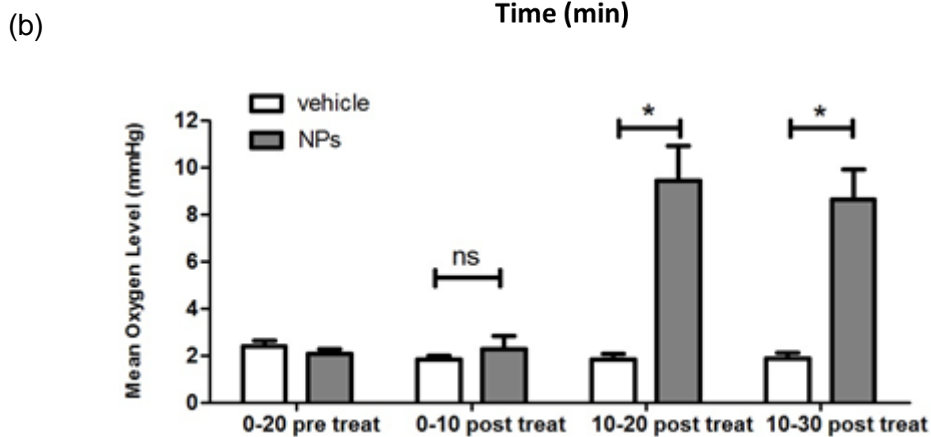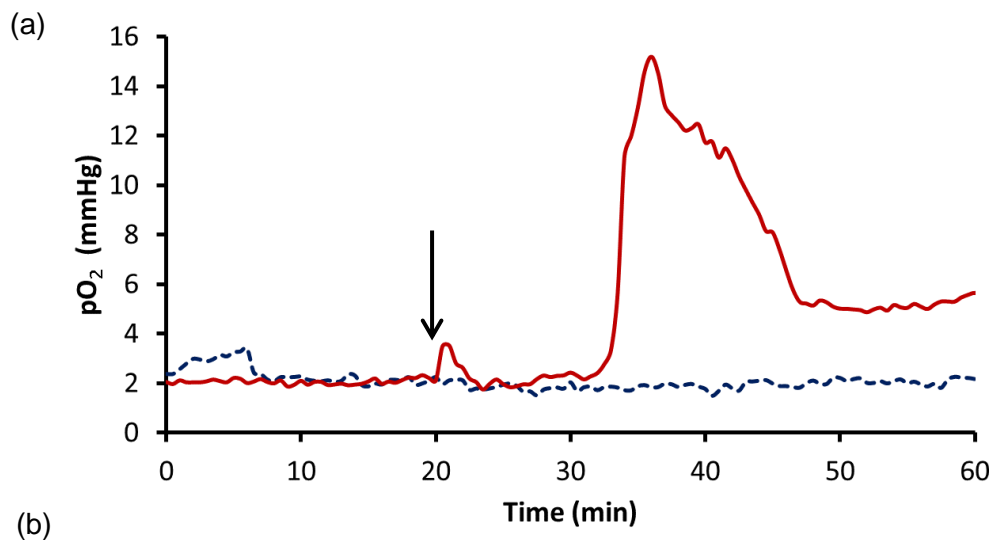
(a)

(b)

Figure 8 (a) Plot of average tumour pO_2 in mice bearing ectopic MIA PaCa-2 pancreatic tumours recorded for 20 min before and 40 min following an IV injection of 1 CaO_2 NPs in a PBS (pH 7.4 ± 0.1) vehicle (red line) or vehicle only (blue dashed line). Arrow indicates when the injection occurred. (b) Plot showing the mean tumour pO_2 for various time intervals before and following IV administration of polymer coated CaO_2 NPs or vehicle only, obtained from integration of the plot shown in (a)., *p≤ 0.05.

The results are shown in Figure 8 and reveal no significant change in the pO_2 reading in the 20 min period before injection for either group with a mean pO_2 reading of ~ 2.0 mmHg. However, approximately 10 min after injection, tumour pO_2 levels in the **1**-CaO_2 NP group increased dramatically reaching a peak of 16 mmHg before levelling off at ~6 mmHg 30 min after injection. In contrast, mice treated with vehicle alone showed no noticeable change in tumour pO_2 over the time course of the experiment.

To put the above results in context, previous studies have indicated that the response to radiotherapy treatment is highly dependent upon tumour oxygenation with an increase from 2.5 mmHg to 6 mmHg significantly affecting loco-regional tumour control in advanced squamous cell head and neck carcinoma.[22] While similar data are not available for PDT, the technique is known to be negatively impacted by hypoxia and the increase in tumour pO_2 levels provided by the **1**-CaO_2 NPs would be expected to have a beneficial effect on PDT mediated efficacy *in vivo*.[23-26] To confirm that this was the case, we treated the same MIA-PaCa-2 tumour model, described in the pO_2 study above, with PDT using a Rose Bengal sensitiser in the presence and absence of the **1**-CaO_2 NPs. Untreated animals and those treated with **1**-CaO_2 NPs alone were used as controls. The NPs were again delivered by IV injection while Rose Bengal was administered by intratumoral injection, to ensure a consistent dose was administered to all of the tumours. Twenty minutes following IV administration of the **1**-CaO_2 NPs, tumours were exposed to light treatment for 3 min. Tumour volume was monitored for 5 days following treatment and the results are shown in Figure 9a. The results demonstrate that there was no significant difference in tumour volume for mice treated with PDT alone or with **1**-CaO_2 NPs alone 5 days after treatment, relative to

the untreated control animals. In contrast, a significant reduction ($p \leq 0.001$) of 70.5 % was observed for animals treated with the **1**-CaO_2 NPs and PDT over the same time period. In addition, there was no significant change in body weight in animals treated with the **1**-CaO_2 NPs alone or in combination with PDT suggesting the treatment was well tolerated (Figure 9b). These results highlight the benefit of **1**-CaO_2 NPs in improving the PDT mediated treatment of hypoxic tumours such as pancreatic adenocarcinoma and may provide benefit in other treatments that are also compromised by hypoxia, most notably radiotherapy.
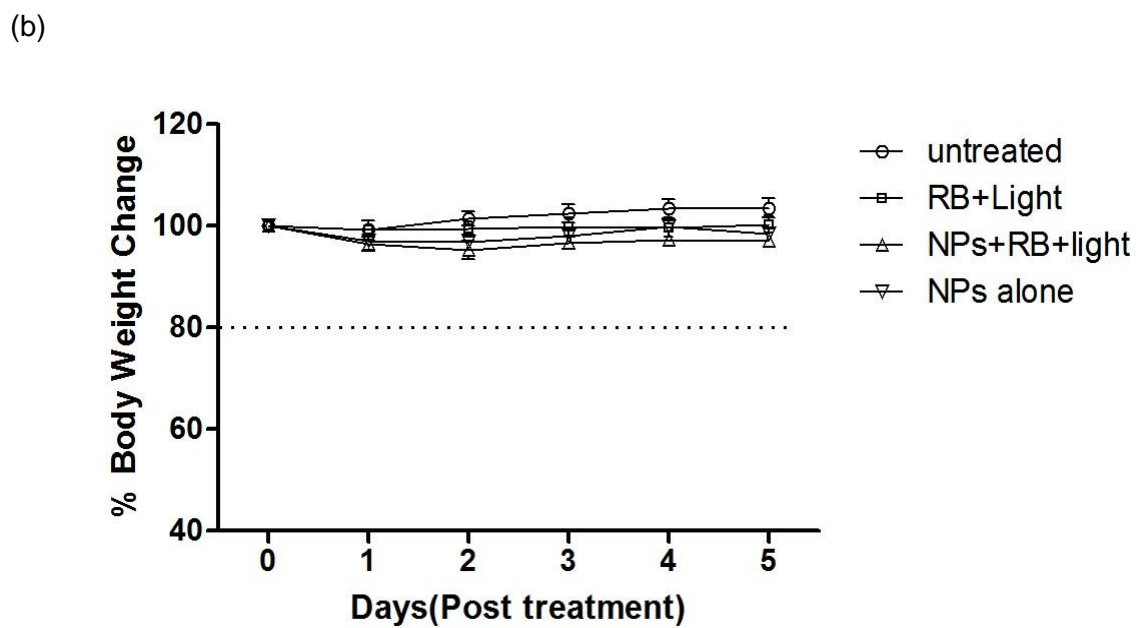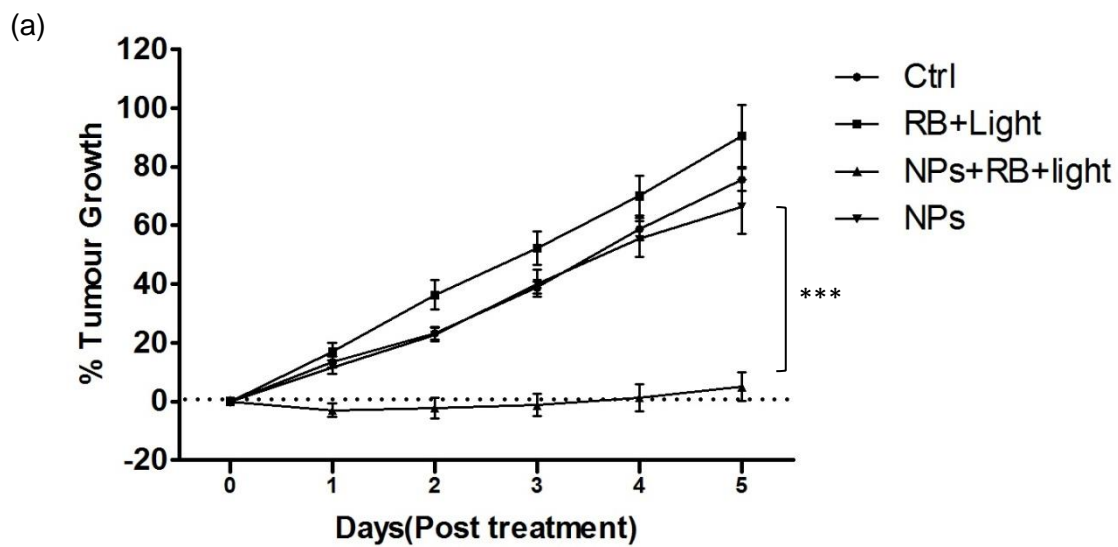
(a)

(b)

Figure 9. (a) Plot of % change in tumour volume against time for SCID mice bearing human xenograft MIA PaCa 2 pancreatic tumours treated with (i) no treatment (squares) (ii) PDT only (circles) (iii) **1**-CaO_2 NPs only (diamonds) and (iv) **1**-CaO_2 NPs and PDT (triangles). (b) Plot of average body weight for each group of mice over the time course of the experiment. ***$p \leq 0.01$.

In summary, we have developed a CaO_2 containing nanoparticle formulation comprising a pH-responsive coating that enables the generation of molecular oxygen in response to changes in environmental pH. Specifically, the polymer coat maintains its integrity when in aqueous solution at pH 7.4, but rapidly dissolves when the pH is lowered to pH 6.2, exposing the CaO_2 particles to water resulting in oxygen generation. The ability of the coated particles to elevate tumour oxygen levels was also demonstrated in mice bearing human xenograft pancreatic tumours where significant elevations in tumour pO_2 were observed 10 mins following IV administration. This increase in tumour pO_2 was also shown to have a dramatic effect on the efficacy of PDT treatment with significant reductions in tumour growth observed in animals that received the coated particles prior to PDT treatment. The utility of this approach is not restricted to PDT but will surely also provide benefit in other treatments that are also negatively impacted by hypoxia.

References

[1]   S. Yano, S. Hirohara, M. Obata, Y. Hagiya, S. Ogura, A. Ikeda, H. Kataoka, M. Tanaka, T. Joh, Current states and future views in photodynamic therapy, Journal of Photochemistry and Photobiology C: Photochemistry Reviews. 12 (2011) 46-67.

[2] S. Cui, D. Yin, Y. Chen, Y. Di, H. Chen, Y. Ma, S. Achilefu, Y. Gu, In vivo targeted deep-tissue photodynamic therapy based on near-infrared light triggered upconversion nanoconstruct, ACS nano. 7 (2012) 676-688.

[3] Taratula, C. Schumann, M.A. Naleway, A.J. Pang, K.J. Chon, O. Taratula, A multifunctional theranostic platform based on phthalocyanine-loaded dendrimer for image-guided drug delivery and photodynamic therapy, Molecular pharmaceutics. 10 (2013) 3946-3958.

[4] A.C. Koong, V.K. Mehta, Q.T. Le, G.A. Fisher, D.J. Terris, J.M. Brown, A.J. Bastidas, M. Vierra, Pancreatic tumors show high levels of hypoxia, International Journal of Radiation Oncology* Biology* Physics. 48 (2000) 919-922.

[5] M. Ilie, N. Mazure, V. Hofman, R. Ammadi, C. Ortholan, C. Bonnetaud, K. Havet, N. Venissac, B. Mograbi, J. Mouroux, High levels of carbonic anhydrase IX in tumour tissue and plasma are biomarkers of poor prognostic in patients with non-small cell lung cancer, Br. J. Cancer. 102 (2010) 1627-1635.

[6] M. Hockel, P. Vaupel, Tumor hypoxia: definitions and current clinical, biologic, and molecular aspects, J. Natl. Cancer Inst. 93 (2001) 266-276.

[7] M. Yoshimura, S. Itasaka, H. Harada, M. Hiraoka, Microenvironment and radiation therapy, BioMed research international. 2013 (2012).

[8] S. Rockwell, I.T. Dobrucki, E.Y. Kim, S.T. Marrison, V.T. Vu, Hypoxia and radiation therapy: past history, ongoing research, and future promise, Curr. Mol. Med. 9 (2009) 442-458.

[9] C. McEwan, S. Kamila, J. Owen, H. Nesbitt, B. Callan, M. Borden, N. Nomikou, R.A. Hamoudi, M.A. Taylor, E. Stride, Combined sonodynamic and antimetabolite therapy for the improved treatment of pancreatic cancer using oxygen loaded microbubbles as a delivery vehicle, Biomaterials. 80 (2016) 20-32.

[10] J.S. Fang, R.D. Gillies, R.A. Gatenby, Adaptation to hypoxia and acidosis in carcinogenesis and tumor progression, 18 (2008) 330-337.

[11] M. Oishi, S. Sumitani, Y. Nagasaki, On− Off Regulation of 19F Magnetic Resonance Signals Based on pH-Sensitive PEGylated Nanogels for Potential Tumor-Specific Smart 19F MRI Probes, Bioconjug. Chem. 18 (2007) 1379-1382.

[12] J. Khodaveisi, H. Banejad, A. Afkhami, E. Olyaie, S. Lashgari, R. Dashti, Synthesis of calcium peroxide nanoparticles as an innovative reagent for in situ chemical oxidation, J. Hazard. Mater. 192 (2011) 1437-1440.

[13] K. Komagoe, T. Katsu, Porphyrin-induced photogeneration of hydrogen peroxide determined using the luminol chemiluminescence method in aqueous solution: A structure-activity relationship study related to the aggregation of porphyrin, Analytical sciences. 22 (2006) 255-258.

[14] S.H. Choi, T.G. Park, G-CSF loaded biodegradable PLGA nanoparticles prepared by a single oil-in-water emulsion method, Int. J. Pharm. 311 (2006) 223-228.

[15] K. Faulkner, I. Fridovich, Luminol and lucigenin as detectors for O2$\dot{s}$−, Free Radical Biology and Medicine. 15 (1993) 447-451.

[16] J. Fuchs, J. Thiele, The role of oxygen in cutaneous photodynamic therapy, Free Radical Biology and Medicine. 24 (1998) 835-847.

[17] Determined from a dose-response experiement conducted using BxPC-3 cells cultured under the conditions described in section 2.5.

[18] R. Sheshala, N. Khan, Y. Darwis, Formulation and optimization of orally disintegrating tablets of sumatriptan succinate, Chemical and Pharmaceutical Bulletin. 59 (2011) 920-928.

[19] M. Doreth, K. Löbmann, H. Grohganz, R. Holm, H.L. De Diego, T. Rades, P.A. Priemel, Glass solution formation in water-In situ amorphization of naproxen and ibuprofen with Eudragit® E PO, Journal of Drug Delivery Science and Technology. 34 (2016) 32-40.

[20] N. Singh, N. Kaur, J. Dunn, R. Behan, R.C. Mulrooney, J.F. Callan, A polymeric sensor for the chromogenic and luminescent detection of anions, European Polymer Journal. 45 (2009) 272-277.

[21] J.W. Wojtkowiak, H.C. Cornnell, S. Matsumoto, K. Saito, Y. Takakusagi, P. Dutta, M. Kim, X. Zhang, R. Leos, K.M. Bailey, Pyruvate sensitizes pancreatic tumors to hypoxia-activated prodrug TH-302, Cancer & metabolism. 3 (2015) 2.

[22] M. Nordsmark, M. Overgaard, J. Overgaard, Pretreatment oxygenation predicts radiation response in advanced squamous cell carcinoma of the head and neck, Radiotherapy and oncology. 41 (1996) 31-39.

[23] Y. Cheng, H. Cheng, C. Jiang, X. Qiu, K. Wang, W. Huan, A. Yuan, J. Wu, Y. Hu, Perfluorocarbon nanoparticles enhance reactive oxygen levels and tumour growth inhibition in photodynamic therapy, Nat. Commun. 6 (2015) 8785.

[24] W. Zhu, Z. Dong, T. Fu, J. Liu, Q. Chen, Y. Li, R. Zhu, L. Xu, Z. Liu, Modulation of hypoxia in solid tumor microenvironment with MnO2 nanoparticles to enhance photodynamic therapy, Advanced Functional Materials. 26 (2016) 5490-5498.

[25] S. Gao, G. Wang, Z. Qin, X. Wang, G. Zhao, Q. Ma, L. Zhu, Oxygen-generating hybrid nanoparticles to enhance fluorescent/photoacoustic/ultrasound imaging guided tumor photodynamic therapy, Biomaterials. 112 (2017) 324-335.

[26] X. Song, L. Feng, C. Liang, K. Yang, Z. Liu, Ultrasound triggered tumor oxygenation with oxygen-shuttle nanoperfluorocarbon to overcome hypoxia-associated resistance in cancer therapies, Nano letters. 16 (2016) 6145-6153.

Figures and Diagrams
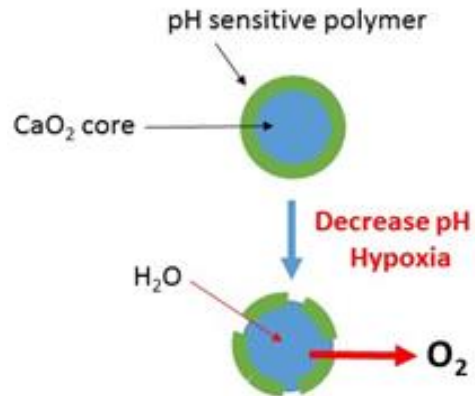
pH sensitive polymer

CaO_2 core

Decrease pH
Hypoxia

H_2O

O_2

Scheme 1 Schematic illustration of how the polymer coat (green) protects the nanoparticle core (blue) from its aqueous environment at normal pH but at lower pH, the polymer coat dissolves, allowing access to the core by water with the resulting generation of oxygen.
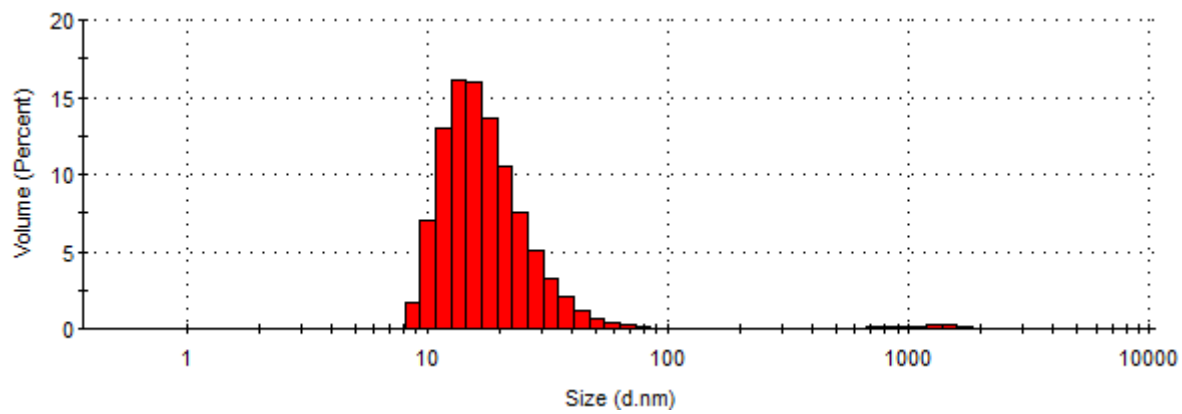
(a)

(b)
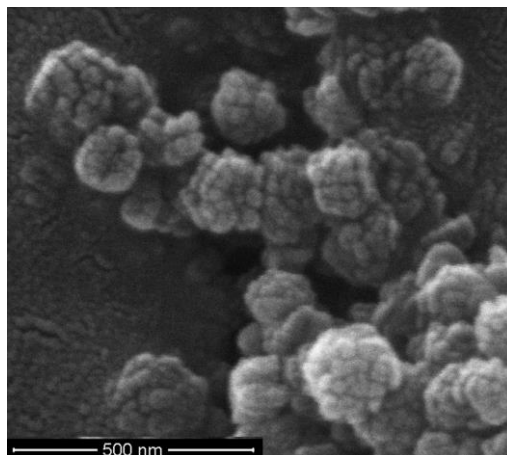
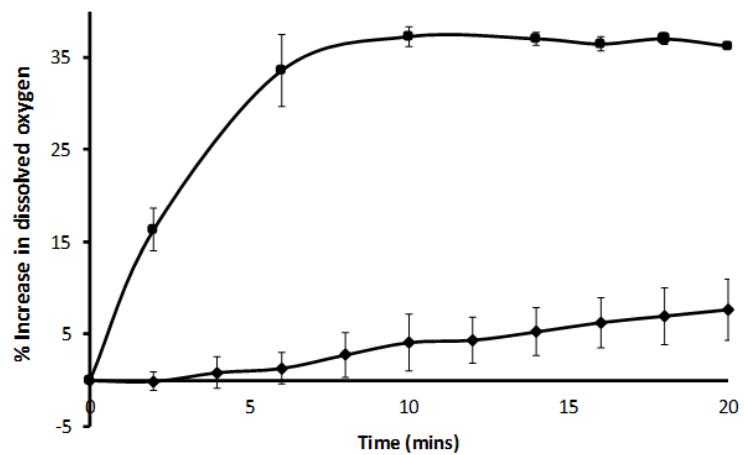**Figure** 1 (a) Representative SEM image and (b) DLS plot of CaO$_2$ NPs.

Figure 2 Plot of % increase in dissolved oxygen against time for a solutions of de-oxygenated PBS with (squares) and without (diamonds) addition of CaO_2 NPs.
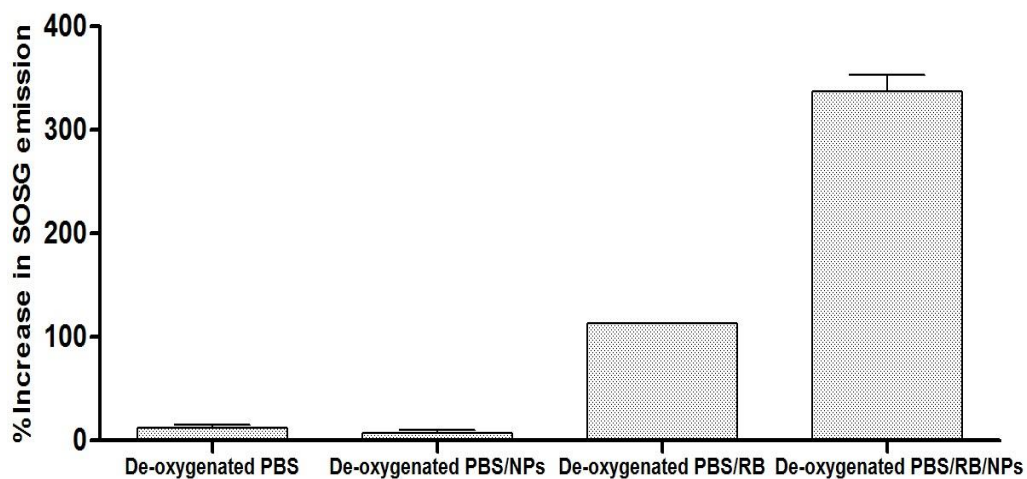
Figure 3 Plot of % increase in SOSG fluorescence at 510 nm for solutions containing (i) degassed PBS (ii) deoxygenated PBS and CaO_2 NPs (iii) deoxygenated PBS and Rose Bengal (RB) and (iv) deoxygenated PBS, Rose Bengal and CaO_2 NPs. Groups (ii)-(iv) also received light treatment.

Figure 4 Plot of cell viability for BxPC-3 cells, cultured under hypoxic conditions with (i) no treatment (CTRL dark bar) or after treatment with (ii) light only (CTRL light bar) (iii) RB only in an EtOH vehicle (RB+EtOH black bar) (iv) RB in an EtOH vehicle + light (RB+EtOH light bar) (v) RB + CaO_2 NP in an EtOH vehicle (RB+NP dark bar) (vi) RB + CaO_2 NP+ light in an EtOH vehicle (RB+NP dark bar).

Figure 5 Stacked ^{1}HNMR spectra of (i) methyl methacrylate (ii) ethyl acrylate (iii) 2-(dimethylamino)ethyl methacrylate and (iv) pH responsive polymer **1**.

(a)

(b)
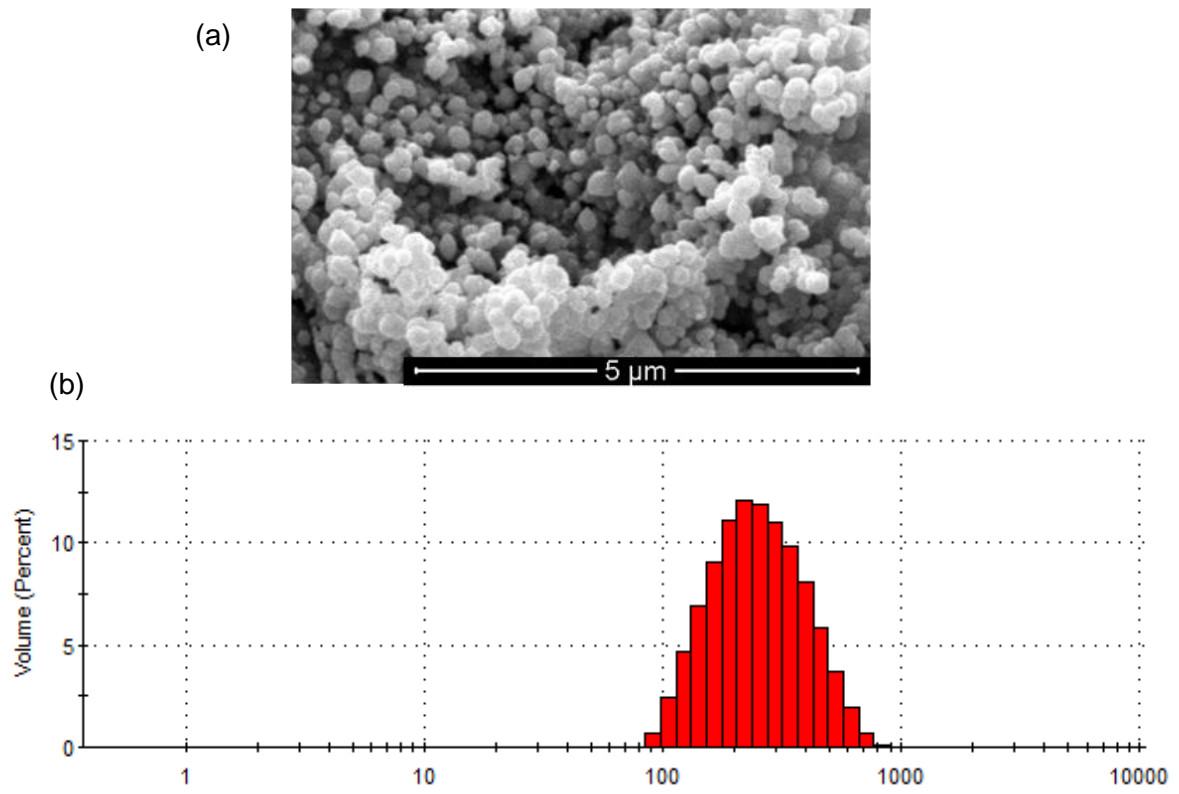
Figure 6 (a) SEM image and (ii) DLS plot of **1**- CaO$_2$ NPs.
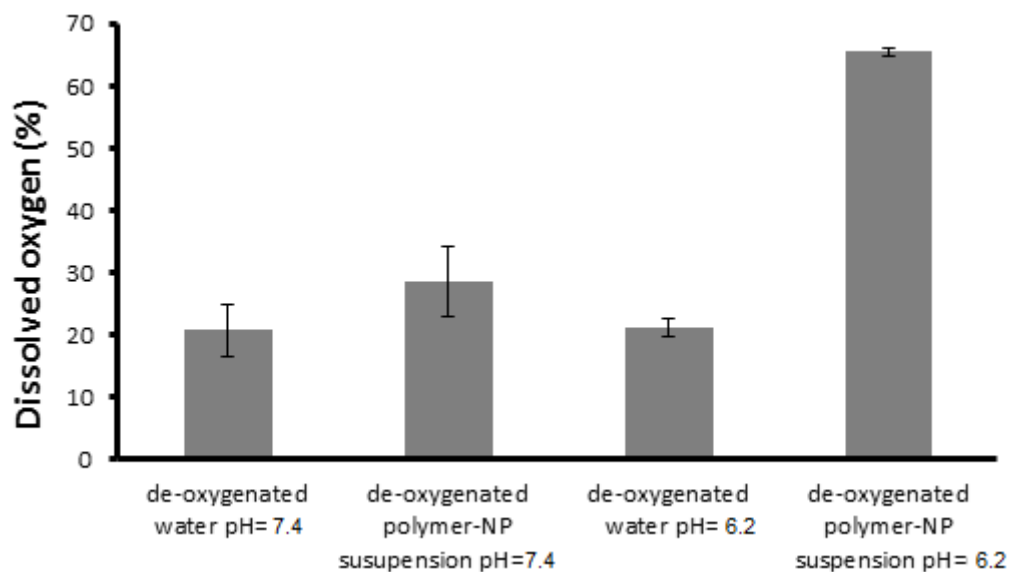
Figure 7 (a) Plot of % dissolved oxygen for solutions of de-oxygenated water at pH 6.2 and pH 7.4 in the absence and presence of **1**-CaO$_2$ NPs. (b) Photographs showing an aqueous suspension of the polymer coated NPs at pH 7.44, 6.88 and 6.19.
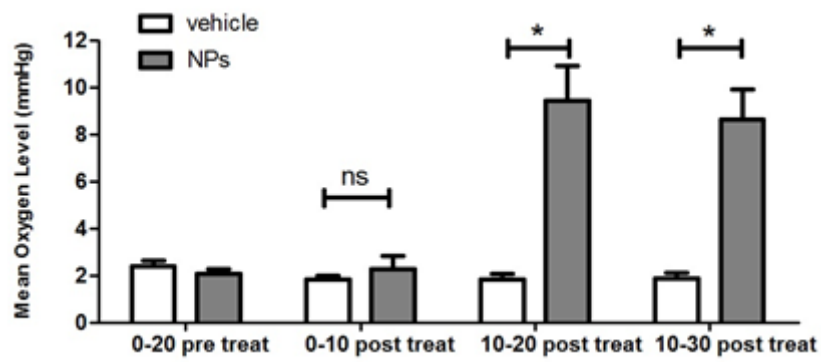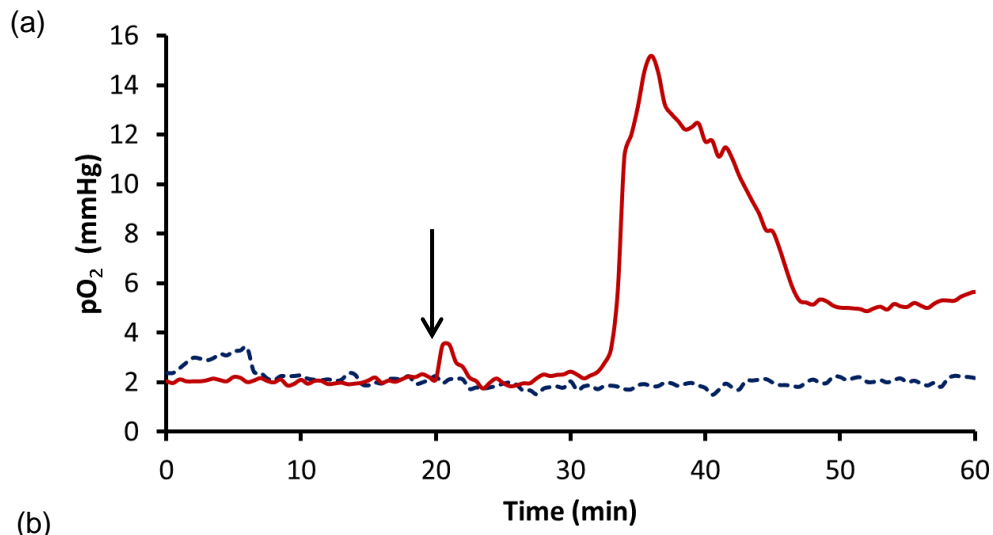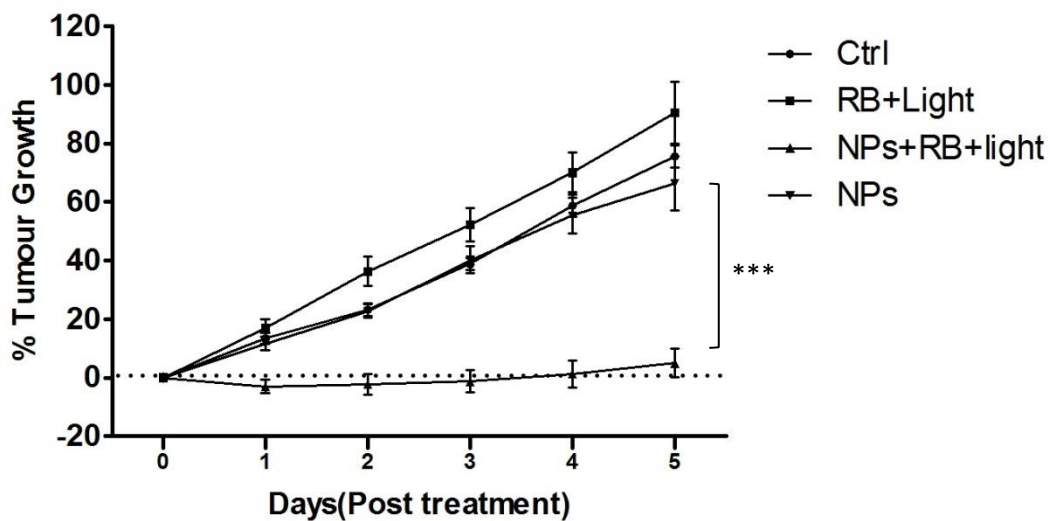
Figure 8 (a) Plot of average tumour pO_2 in mice bearing ectopic MIA PaCa-2 pancreatic tumours recorded for 20 min before and 40 min following an IV injection of 1 CaO_2 NPs in a PBS (pH 7.4 ± 0.1) vehicle (red line) or vehicle only (blue dashed line). Arrow indicates when the injection occurred. (b) Plot showing the mean tumour pO_2 for various time intervals before and following IV administration of polymer coated CaO_2 NPs or vehicle only, obtained from integration of the plot shown in (a)., *p≤ 0.05.
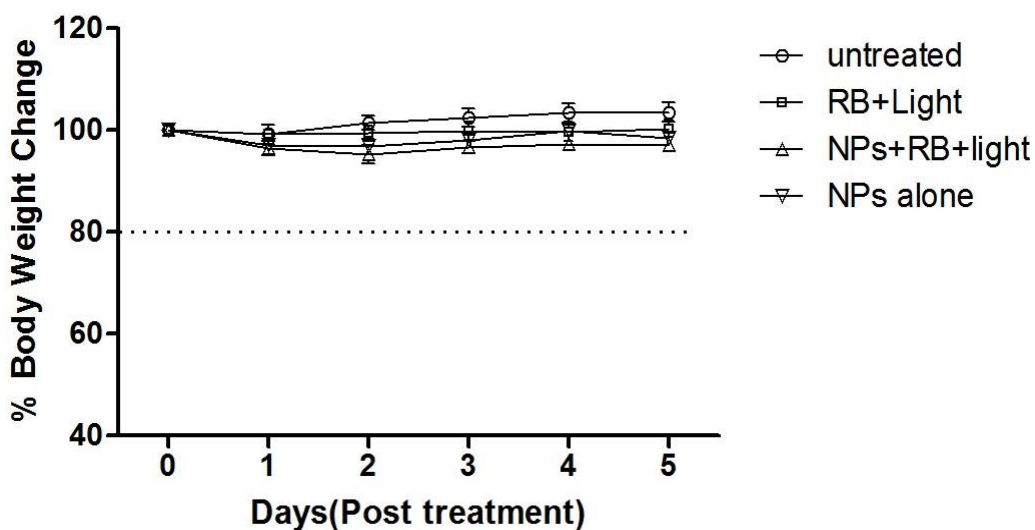
Figure 9. (a) Plot of % change in tumour volume against time for SCID mice bearing human xenograft MIA PaCa 2 pancreatic tumours treated with (i) no treatment (squares) (ii) PDT only (circles) (iii) **1**-CaO_2 NPs only (diamonds) and (iv) **1**-CaO_2 NPs and PDT (triangles). (b) Plot of average body weight for each group of mice over the time course of the experiment. ***$p \leq 0.01$.